

# Pigment Identification of Ortelius' Historical Maps using Hyperspectral Imaging

Zealandia S. N. Fatma, Hilda Deborah, and Jon Y. Hardeberg; Department of Computer Science, Norwegian University of Science and Technology; Gjøvik, Norway

Eleftherios Papachristos; Department of Design, Norwegian University of Science and Technology; Gjøvik, Norway

## Abstract

*Hyperspectral imaging (HSI) has been widely used in the conservation studies of various cultural heritage (CH) objects, e.g., paintings, murals, and handwritten historical manuscripts. In this work, HSI is used to study painted historical maps, i.e., five maps of the Scandinavia region from the Ortelius collection preserved at the National Library of Norway in Oslo. Given knowledge of their colour application and usage, HSI-based pigment identification is performed, assuming several spectral mixing theories, i.e., pure pigments, subtractive, and additive mixing models. The obtained results are discussed, showing both the pure pigment and subtractive mixing model to be suitable for pigment identification in the case of watercolour applied on paper substrate.*

## Introduction

Hyperspectral imaging (HSI) is a process to obtain spectral resolution imagery through contiguous narrow bands across the electromagnetic spectrum, typically extends from visible spectrum (0.4 to 0.7  $\mu\text{m}$ ) to the shortwave infrared (SWIR) range (about 2.5  $\mu\text{m}$ ) [1]. Its use has now become quite popular in conservation studies of cultural heritage (CH) objects since it enables a non-invasive approach to perform, e.g., pigment identification, using non-visible information that could not typically be observed by other techniques, e.g., colorimetry. Studies using HSI for parchments [2], paintings [3], and murals [4] have been conducted, demonstrating its ability to identify pigments or colourants of various types of CH artefacts.

In the use of HSI for conservation studies, historical maps or atlases remained relatively unexplored, despite them also demonstrating rich coloured materials and, therefore, colour history. These maps and atlases will also enable more complex HSI-based analyses compared to other CH objects. Not only that they demonstrate the intricacies of the physical variability of coloured materials, but the semantic meaning of colours will provide necessary context and constraints for analysis and processing. This contrasts with, e.g., paintings, where the paint layers applied to a canvas is mostly of artistic expressions and techniques and less of a function, such that the exact proportion or concentration of materials at each pixel is often of interest. The complex relationship between colour and maps is described by Lange [5] as a communication tool between cartographer or mapmaker to their audiences. Cartographers carefully choose the system of colour usage in their map products to effectively communicate information they want to deliver. Through times, this system also reflects how colours are used in each period, the change of physical and political landscapes of a geographical region, printing technology, and the evolution of the colourant itself.

In this work, we study five historical maps of the Scandinavia region from the Ortelius collection preserved at the National Library of Norway in Oslo. Focus is given to thirteen red pigment samples from the maps, which can be divided into three objects of interests, i.e., fantasy creature, lands, and castles. Three assumptions of the nature of the colour mixing are taken and compared. They are the assumptions of pure pigments and two mixing models allowing to account for the paper substrate, i.e., additive and subtractive models. Using a spectral library of pure pigments [6], a target pixel is reconstructed and the result is compared using Spectral Angle Mapper (SAM) [7]. This work is a continuation of a previously conducted pilot study focusing on one of the Scandinavia maps [7], where pure pigments assumption was taken to study five colours, i.e., yellow, orange, green, red, and pink.

## Data and Methods

The focus of this study is five maps of Scandinavia from the Ortelius collection, originating from the period between 1570 and 1603 [8], all part of the Ortelius atlas and map collection housed at the National Library of Norway in Oslo. Each map sheets were produced by copper plate printing and manually coloured in later period by hired colourists. While the dating for each map is of the printing production and the dating for when they were coloured is unknown, quoting Primeau in Ref. [9] “[...] the practice of colouring prints was common during the Renaissance and Baroque eras and that modern questions about the vintage of the colouring are often unfounded.” Upon visual observation, we can see that each map sheet displays the region of Scandinavia in different colours. For example, in Figure 1, the map code 7-746 that was produced in



**Figure 1.** Parts of the maps used in this study, (left) map sheet code 7-746, and (right) 5-738.

1575 shows that the whole Scandinavia area (now Denmark, Norway, and Sweden) was coloured in pink. In the next period, 1588, the same region now appeared in different colours in the map code 5-738. This observation illustrates why the pigment identification for this map collections is an important information for further history and cartography analyses. Aiming to identify the pigments, in the following we elaborate the data and methods used.

## Data

In this study, we use two HSI datasets, i.e., the target and reference materials. The target data, which is our main object of study, is the hyperspectral images of the Scandinavia maps. Then, a spectral library of Kremer pure pigments [6] is used as the reference material in the pigment identification process.

### Target: Scandinavia Maps of Ortelius atlas

From the five maps used in this study, we narrow down our focus to three object types: geographical objects (castle/city and land) and fantasy creatures, and only those coloured in red. The hyperspectral images were previously acquired in Deborah, *et al.* [7], where Specim IQ hyperspectral camera was used to do the primary data acquisition which was performed in a controlled environment, where the light source can be assumed to be scattered evenly in all directions of the map surface, or diffuse illumination. The data are given in the format of spectral reflectance, with values ranging between 0 and 1. Spectrally, it is composed of 204 bands covering the spectral range 397.32-1003.58 nanometers (nm) in 3.09 nm interval between bands. Due to noise, only 200 bands from 405.97-1000.49 nm are used. From a total of 71 hyperspectral images, we selected 13 regions of interests (ROIs), each of 5x5 pixel size. These ROIs consist of 5 castles (dark red colours), 7 land (ranging from dark red to orange-ish colours), and 1 fantasy creature (dark red) samples. These samples were selected to represent different variations of red within the selected map sheets.

The average reflectance spectra of the 13 ROIs are shown in Figure 2. Paying close attention to the spectra, it is noticeable that two samples, i.e., 071\_138 and 071\_265, are likely mixed with a green pigment since each shows a peak located between the 400-500 nm region. Figure 3 confirms this, where the red pigments/ samples are likely layered above a diluted wash of green of the larger region in its surrounding.

### Reference: Kremer pure pigment spectral library

The used Kremer spectral library was acquired using Hypslex VNIR-1800 line scanner, which captures 1800 pixels/line, in the range 405.369 to 995.827 nm with a sampling spectral interval of 3.26 nm [6]. The total number of bands for each spectral reflectance signal is 186. This spectral library contains various categories, for example, organic and inorganic as well as modern and historical pigments. As a note, only a part of the whole spectral library is used, i.e., part containing Kremer-made and historical pigments, to exclude most modern pigments from the search space. The spectral library is represented in terms of spectral reflectance values between 0 and 1. Because the two data, i.e., target and reference, are in different spectral resolution, a 1D interpolation is needed before further data processing. We interpolated the 186 bands of the Kremer spectral library to the map hyperspectral images, resulting in 200 bands for each Kremer pigment spectral reflectance.

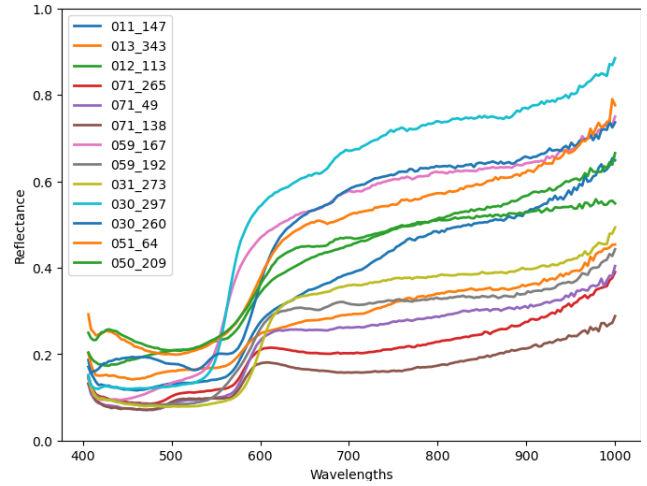


**Figure 2.** Reflectance spectra of the 13 samples used in this study, consisting of the average spectra of ROIs taken from 5 castle, 7 land, and 1 fantasy creature objects within the five maps.



**Figure 3.** Samples 071\_138 (left) and 071\_265 (right) representing castle objects, with their respective ROIs indicated inside the white squares. These red samples might be mixed with the underlying green colour used to represent the geographical Land object.

## Method

To perform pigment identification, first, we take the average spectral reflectance values of each ROI (5x5 pixel size). Then, we experimented with three approaches: (i) pure pigment, (ii) subtractive mixing model, and (iii) additive mixing model. The pure pigment approach assumes that the selected ROIs can be directly used to obtain the pigment spectral information without significant interference from the reflectance of the paper substrate. This can be expressed below, where  $Y$  is an observed average signal from the selected ROIs and  $\rho$  is a match from the Kremer library. In other words, the observed signal is equal to the signal of a pure pigment.

$$Y = \rho \quad (1)$$

The subtractive method is used under the assumption of the final observed reflectance being the result of the interaction between the optical properties of a pigment and the paper substrate. In remote sensing, this method is considered a nonlinear mixture model [10], studied from the following scenario: a single vegetation layer above soil results in multiple scattering effect. In this study, we consider the use of this method as similarly describing the interaction between the paper and the pigment layer above. This method is expressed using an arithmetic multiplication between the individual pigment reflectance values and the paper substrate. The reflectance

value of the paper was taken for each map from their uncoloured surfaces. Below is the original equation for subtractive model [11]:

$$Y = \prod_{i=1}^q \rho_i^{\alpha_i} \quad (2)$$

where the observed average reflectance value  $Y$  is said to be the product of multiplying all the individual factors of  $\rho$  of concentration  $\alpha$ . In this context,  $\rho$  is the spectral reflectance values of a Kremer pigment and the corresponding paper substrate.

The additive model is also known as linear model; it has been widely used in remote sensing. This concept is based on the optical mixing interaction within a pixel as captured by the sensor of a satellite, where every object does not interact with each other in a such way that would change the individual spectral properties. By using this method, we assume that the mixing between the paper and watercolour layer in the maps to be like the above optical blending case in remote sensing. Below is the additive model equation [11].

$$Y = \sum_{i=1}^q \rho_i \alpha_i \quad (3)$$

Compared to the previous approach, here,  $Y$  is the result of the addition of a Kremer pigment and the paper spectral reflectance values, each multiplied by its abundance (proportion) within a single pixel. In our study, we assume equal abundance for both the pigment and paper.

Spectral Angle Mapper (SAM) is then used to find the closest match between an observed signal and its reconstruction using either of the three approaches described in equations (1-3). The algorithm has been widely used in remote sensing particularly for supervised image classification for both multispectral and hyperspectral [12], by using the reflectance vector value of reference and target spectra. This algorithm compares the similarity between target and reference spectra by calculating arccosine of  $\alpha$  angle between target spectrum to a reference in  $n$ -D space, where  $n$  is the number of bands. Below is the SAM equation [13]:

$$SAM = \cos^{-1} \left( \frac{\sum_{i=1}^{nb} t_i r_i}{\left( \sum_{i=1}^{nb} t_i^2 \right)^{\frac{1}{2}} \left( \sum_{i=1}^{nb} r_i^2 \right)^{\frac{1}{2}}} \right), \quad (4)$$

where  $t$  = target or observed colour pigment  
 $r$  = reference or Kremer pure pigment spectra  
 $nb$  = number of bands

Smaller arccosine of  $\alpha$  angle represents the closer matches spectra shape similarity to the reference. As previously mentioned in Section Data, one dimensional interpolation is performed prior to this step due to the difference in spectral dimension between the target and reference spectra.

## Experimental Design

In this study, we tested the three-pigment identification approaches to find the most similar Kremer spectral reflectance, i.e., assuming pure pigments, the subtractive, and additive mixing models. For each approach, three Kremer pigments with the lowest SAM values are obtained as candidate solutions. The flowchart of the experiment is shown in Figure 4. Descriptive analysis and statistical analysis are included to understand the result.

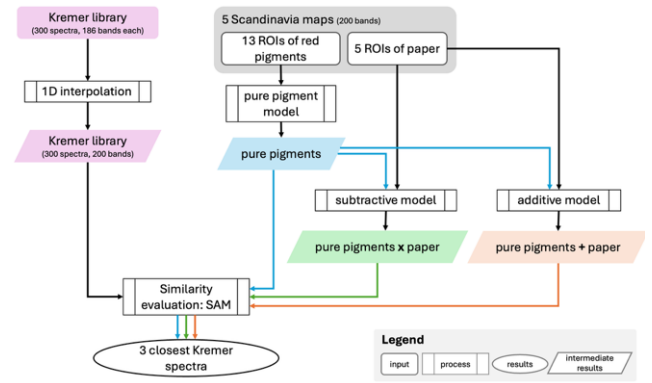


**Figure 4.** The study's experimental design, showing three models of pigment identification, i.e., pure pigment, subtractive, and additive models. Thirteen HSI samples were obtained from five Scandinavia maps, along with their respective paper reflectance samples. The paper reflectances are used for subtractive and additive models. To find the closest Kremer reflectance, SAM equation is applied to the results of each model, and three Kremer spectra are given.

## Result and Discussion

Comparison of the best candidate matches having the lowest SAM score returned by each approach for each sample can be seen in Figure 5. For samples taken from the Fantasy Creature and Land objects, the additive mixing model always results in a pigment with higher SAM value, almost always significantly so. The spectral reflectance and their first derivative of these candidate matches for a sample taken from a Land object, i.e., 030\_297, can be seen in Figure 6. The candidate pigment by the additive approach is clearly the least similar since its slope is the furthest shifted from the slope of the target pigment. This shift is clearer when visualized in the first derivative form, where we can see the peak of the additive model's solution is the furthest away from that of the target. Since in most cases the additive mixing model suggests candidate matches with significantly higher SAM values, it will not be considered any further in this discussion section.

As seen in Figure 5, the most similar matches for the object category Land are dominated by matches suggested by the pure pigment approach, while the Castle category by the subtractive mixing model. This pattern can be explained by looking into the characteristics of how the watercolour pigments were applied to the paper substrate in the two different categories. On object category Land, it tends to be of one diluted wash of a single colour or more around the edges of a geographical region. The category Land, on the other hand, will be a concentrated colour applied on top of the diluted wash, potentially resulting in pigment mixing. See examples in Figure 3, where the Land category here is coloured in green. Based on such observations, we can assume that the pure pigment assumption can be considered for when diluted wash of watercolour is applied. Meanwhile the subtractive method suggests sensitivity to possibly multiple layers of different colours or pigments, thus possible pigment mixing. The samples shown in Figure 3, and subsequently their spectra in Figure 2, are samples with the lowest similarities within the object category. Considering that the Kremer library is a library of pure pigments, these results are understandable

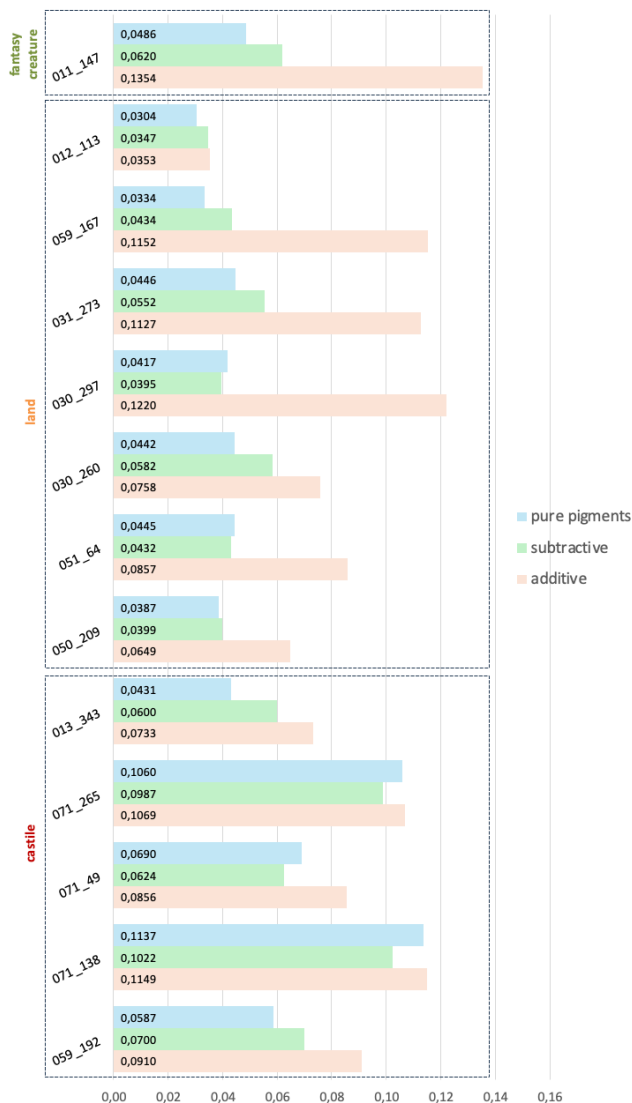


**Figure 5.** Comparison of the lowest SAM values returned by each method and for each sample pigment, grouped by the object category. In general, the additive model almost always returns significantly the least similar match than the pure pigment and subtractive model.

since the best candidates are simply not found. Further experiment can be performed using the subtractive mixing model, whereby we should consider not only mixing between the paper and red target, but also with the green colourant surrounding the samples.

Three most similar candidate pigment matches were also identified for the two methods, totalling to 52 candidate matches. Their list, grouped by the object type and approach, can be seen in the Supplementary Table A-1. The overall SAM values indicate high similarity match between the maps' red pigments and the available Kremer spectral library data, ranging from 0.0304 as the highest and 0.1173 as the lowest similarity. As a reminder, these candidates were only selected from Kremer-made historical pigments category within the entire spectral library. From these

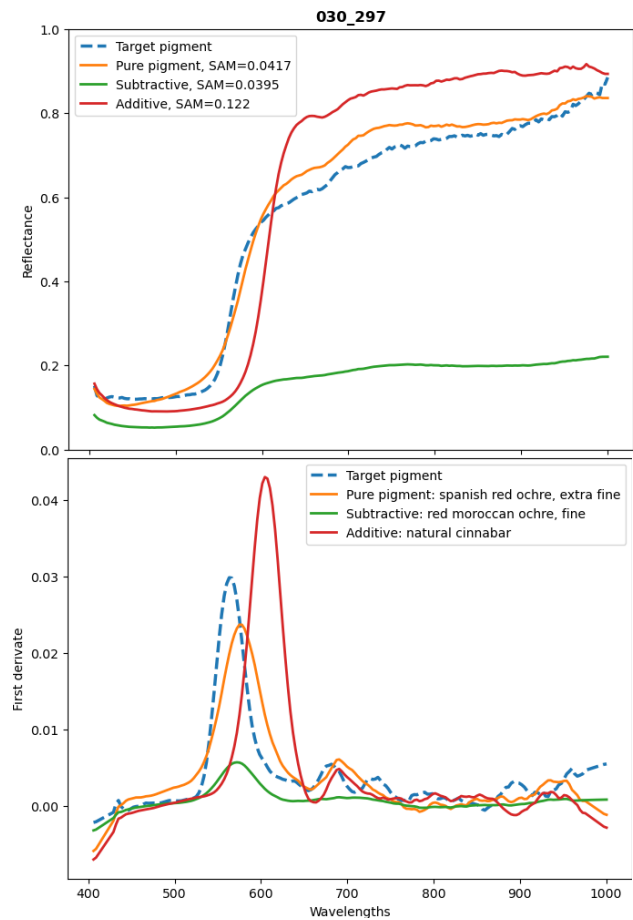


**Figure 6.** The best candidate matches returned by all three approaches for sample 030\_297 taken from Land object, shown in its spectral reflectance and the first derivative of the reflectance forms.

suggested pigments, a process of narrowing down the pigment families was conducted with conservators from the National Library in Oslo and through literature study to consider the historical perspectives of pigments. Among these candidate matches, the following pigment families historically fits the production period of each map in the 15<sup>th</sup> and 16<sup>th</sup> centuries, i.e., red and brown ochres, madder lake, and cinnabar. Other pigments such as Snaefellsjokull red (mineral pigment from Iceland) and pinkcolor (modern pigment invented in the 19<sup>th</sup> century) are unlikely candidate.

## Conclusion and Future Works

This study showed the use of HSI to identify the pigments or colorants of historical maps, specifically Scandinavia maps from Ortelius atlas collection. Five map sheets originating from between 1570 and 1603 were used, with a focus on their red colours. The total samples that we observed are 13, taken from objects of fantasy creature, land, and castle. Three approaches were used to identify the pigments over the object categories: assuming pure pigment, subtractive, and additive mixing models; each selected to demonstrate a distinct way how pigments spectra interact optically. The subtractive mixing model indicates the sensitivity to subtle colour variations, even within the same type of object. This suggests



that it considers the effect of pigment mixing and layering, as indicated by the SAM values of its suggested matches for the samples within object category Castle. The additive mixing model is not to be considered further for this case of watercolour, especially as it consistently suggests matches with significantly higher SAM values compared to the subtractive model and pure pigment methods. A discussion with conservators and literature review were conducted to narrow down the selection from the suggested candidates, to consider the pigments' historical perspective. As a result, thus far, the following are pigment families identified in the maps: red ochre, brown ochre, madder lake, and cinnabar. These pigments fit the map production period, between the 15<sup>th</sup> and 16<sup>th</sup> centuries. Other more modern pigment candidates need to be observed further by including XRF analysis. To conclude, in a pigment identification study, HSI analysis needs to be accompanied with other supporting analysis (e.g., XRF) as part of a whole multimodal analysis for watercolour pigments. Nevertheless, this work shows the mixing model to choose in the case of watercolour applied on paper, for the Scandinavian maps of Ortelius atlas.

## References

- [1] A. Gary Shaw and K. Burke Hsiao-hua, 'Spectral Imaging for Remote Sensing', *Lincoln Laboratory Journal*, vol. 14, no. 1, pp. 3–28, 2003.
- [2] D. Bai, D. W. Messinger, and D. Howell, 'A pigment analysis tool for hyperspectral images of cultural heritage artifacts', presented at the SPIE Defense + Security, M. Velez-Reyes and D. W. Messinger, Eds., Anaheim, California, United States, May 2017, p. 101981A. doi: 10.1117/12.2261852.
- [3] H. Deborah, S. George, and J. Y. Hardeberg, 'Spectral-divergence based pigment discrimination and mapping: A case study on *The Scream* (1893) by Edvard Munch', *Journal of the American Institute for Conservation*, vol. 58, no. 1–2, pp. 90–107, Apr. 2019, doi: 10.1080/01971360.2018.1560756.
- [4] Z. Gao, M. Du, N. Cao, M. Hou, W. Wang, and S. Lyu, 'Application of hyperspectral imaging technology to digitally protect murals in the Qutan temple', *Heritage Science*, vol. 11, no. 1, p. 8, Jan. 2023, doi: 10.1186/s40494-022-00847-7.
- [5] D. Lange and B. van der Linde, Eds., *Maps and colours: a complex relationship*. in Mapping the past, no. volume 3. Leiden ; Boston: Brill, 2024.
- [6] H. Deborah, 'Hyperspectral Pigment Dataset', in *2022 12th Workshop on Hyperspectral Imaging and Signal Processing: Evolution in Remote Sensing (WHISPERS)*, Rome, Italy: IEEE, Sep. 2022, pp. 1–5. doi: 10.1109/WHISPERS56178.2022.9955067.
- [7] H. Deborah, C. Palandri, and G. Oretti, 'Estimating the Color Palette of Ortelius' Atlas: A Case Study of Hyperspectral Imaging for Rapid Pigment Screening', in *2023 13th Workshop on Hyperspectral Imaging and Signal Processing: Evolution in Remote Sensing (WHISPERS)*, Athens, Greece: IEEE, Oct. 2023, pp. 1–5. doi: 10.1109/WHISPERS61460.2023.10430960.
- [8] M. P. R. van den Broecke, *Ortelius atlas maps: an illustrated guide*. MS 't Goy: HES Publ, 1996.
- [9] T. Primeau, 'The Materials and Technology of Renaissance and Baroque Hand-Colored Prints', in *Painted Prints: The Revelation of Color in Northern Renaissance & Baroque Engravings, Etchings & Woodcuts*, Pennsylvania State University Press, 2002, pp. 49–78.
- [10] J. M. P. Nascimento and J. M. Bioucas-Dias, 'Nonlinear mixture model for hyperspectral unmixing', presented at the SPIE Europe Remote Sensing, L. Bruzzone, C. Notarnicola, and F. Posa, Eds., Berlin, Germany, Sep. 2009, p. 74770I. doi: 10.1117/12.830492.
- [11] F. Grillini, J.-B. Thomas, and S. George, 'Comparison of Imaging Models for Spectral Unmixing in Oil Painting', *Sensors*, vol. 21, no. 7, p. 2471, Apr. 2021, doi: 10.3390/s21072471.
- [12] Rashmi S, Swapna Addamani, Venkat, and Ravikiran S, 'Spectral Angle Mapper Algorithm for Remote Sensing Image Classification', *IJISSET*, vol. 1, no. 4, pp. 201–205, Jun. 2014.
- [13] F. A. Kruse *et al.*, 'The spectral image processing system (SIPS)—interactive visualization and analysis of imaging spectrometer data', *Remote Sensing of Environment*, vol. 44, no. 2–3, pp. 145–163, May 1993, doi: 10.1016/0034-4257(93)90013-N.

## Author Biography

*Zealandia S. N. Fatma is Ph.D. student at the Colourlab, Department of Computer Science, NTNU with a background in remote sensing and cartography. Her Ph.D. research focuses on the interactive visualisation of hyperspectral images in an exhibition setting, specifically for a collection of cultural heritage maps and atlases.*

*Hilda Deborah is Senior Researcher at the Colourlab, Department of Computer Science, Norwegian University of Science and Technology (NTNU). She received her PhD in Computer Science from NTNU and in Image and Signal Processing from the University of Poitiers in 2016. Besides her expertise in more fundamental image processing and spectral imaging, she also has interests in digital humanities and human-computer interaction, driven by her passion for making science accessible to public.*

*Jon Y. Hardeberg is Professor of Colour Imaging at the Colourlab at NTNU - Norwegian University of Science and Technology. His research interests include spectral imaging, image quality, material appearance, and cultural heritage imaging, and he has co-authored over 300 publications. He has coordinated three European MSCA ITN projects (CP7.0, ApPEARS, CHANGE). and started two companies, Artikolor AS and Spektralion AS, to disseminate and apply knowledge and tools in art history, colour, and spectral imaging.*

*Eleftherios Papachristos is Associate Professor at the Department of Design, NTNU with a research focus on Human-Centred AI and Interaction Design. He is especially interested in the intersection of artificial intelligence and interaction design, investigating how advances in AI are changing the way we interact with technology.*

**Supplementary Table A-1.** This table shows three Kremer pigment candidates having the smallest SAM values, as suggested by the method assuming pure pigment and the subtractive mixing model. Each sample row contains the name of Kremer candidate and its corresponding SAM value, ranked 1 to 3 from the most to less similar pigments.

sample	object	pure pigment			subtractive		
		1	2	3	1	2	3
011_147	fantasy creature	snaefellsjoekull red	brown earth from Otranto	brown earth from Otranto	snaefellsjoekull red	madder lake made of roots, dark red	snaefellsjoekull red
		0.0486	0.0628	0.0699	0.0620	0.0625	0.0630
012_113	land	iseo brown	brown-red slate	red jasper	pinkcolor	pinkcolor	pinkcolor
		0.0304	0.0325	0.0392	0.0347	0.0355	0.0438
050_209		snaefellsjoekull red	madder lake carmine red	cote d'azur violet	pinkcolor	pinkcolor	pinkcolor
		0.0387	0.0448	0.0465	0.0399	0.0419	0.0518
030_260		madder lake made of roots, dark red	burgundy red ochre, fine	madder lake, genuine	pinkcolor	madder lake, genuine	madder lake, genuine
		0.0442	0.0448	0.0470	0.0582	0.0588	0.0598
051_64		snaefellsjoekull red	snaefellsjoekull red	madder lake, genuine	madder lake carmine red	madder lake, genuine	pinkcolor
		0.0445	0.0511	0.0544	0.0432	0.0442	0.0574
031_273		cinnabar, fine	natural cinnabar	cinnabar, fine	cinnabar, fine	natural cinnabar	burgundy red ochre, fine
		0.0446	0.0494	0.0524	0.0552	0.0638	0.0665
059_167		Spanish red ochre, extra fine	Spanish red ochre, extra fine	red Moroccan ochre, fine	realgar, genuine	yellow ochre, from Andalusia	realgar, genuine
		0.0334	0.0484	0.0512	0.0434	0.0446	0.0458
030_297		Spanish red ochre, extra fine	Spanish red ochre, extra fine	red Moroccan ochre, fine	red Moroccan ochre, fine	Spanish red ochre, extra fine	red jasper
		0.0417	0.0421	0.0427	0.0395	0.0443	0.0501
013_343	castle	snaefellsjoekull red	cote d'Azur violet	cote d'Azur violet	bistre	gray from mels	ivory black, genuine
		0.0431	0.0471	0.0532	0.0600	0.0645	0.0663
059_192		red Moroccan ochre, fine	Spanish red ochre, extra fine	burgundy red ochre, fine	red jasper	Spanish red ochre, extra fine	pinkcolor
		0.0587	0.0649	0.0666	0.0700	0.0743	0.0760
071_49		brown ochre, from Andalusia	brown earth from otranto	red Moroccan ochre, fine	red jasper	Spanish red ochre, extra fine	red jasper
		0.0690	0.0706	0.0721	0.0624	0.0709	0.0729
071_138		black earth, from Andalusia	rhodonite black	rhodonite black	aegirine, fine	bistre	aegirine, fine
		0.1137	0.1171	0.1173	0.1022	0.1063	0.1068
071_265		rhodonite black	rhodonite black	black earth, from Andalusia	bistre	bistre	ivory black, genuine
		0.1060	0.1065	0.1079	0.0987	0.1020	0.1029